Response of Fibroblasts to Transforming Growth Factor-β1 on Two-Dimensional and in Three-Dimensional Hyaluronan Hydrogels

Xia Chen, M.D., Ph.D., and Susan L. Thibeault, Ph.D.

Transforming growth factor-β1 (TGF-β1), an important cytokine with multiple functions, is secreted during wound healing. Previous studies have utilized two-dimensional (2D) cell culture to elucidate the functions of TGF-β1; however, 2D culture does not represent the complex three-dimensional (3D) *in vivo* environment. Using a synthetic hyaluronan (HA) extracellular matrix (ECM) hydrogel, we investigated the effect of TGF-β1 on fibroblasts cultured in three conditions—on tissue culture polystyrene (TCP), on HA (2D), and in HA (3D). After TGF-β1 treatment (0.1 to 20 ng/mL), morphological features and ECM regulation were analyzed by immuno-cytochemistry, Western blot, quantitative polymerase chain reaction, and zymogram assays. On TCP, cells showed the typical spindle shape with strong alpha smooth muscle actin (α-SMA) staining of cytoplasmic myofilaments along the cell axes after TGF-β1 treatment; on HA (2D), spindle-shape cells showed little α-SMA staining; in HA (3D), cells were smaller and rounded with less α-SMA deposition. The α-SMA gene and protein expression on TCP were significantly upregulated by TGF-β1, but TGF-β1 did not induce *α-SMA* expression in the presence of HA (both 2D and 3D). 3D HA culture significantly downregulated collagen I, III, and fibronectin expression, increased matrix metalloproteinase 1 and 2 (MMP1/MMP2) activity, upregulated *MMP1* mRNA and downregulated *TIMP3* mRNA expression. This study suggested that exogenous HA, particularly in 3D culture, appears to suppress ECM production, enhances ECM degradation and remodeling, and inhibits myofibroblast differentiation without decreasing TGF-β receptor expression.

Introduction

WOUND HEALING IS A COMPLEX PROCESS that involves inflammation, proliferation, and remodeling. Throughout each of these phases there are dynamic, reciprocal interactions between the extracellular matrix (ECM), growth factors, and cells[1] as the tissue attempts to regenerate.[2] Transforming growth factor β1 (TGF-β1) plays a crucial role in aberrant healing.[3–8] *In vivo*, TGF-β1-mediated chemotaxis has been shown to promote fibroblast proliferation and recruitment to the wound bed, synthesis of ECM, while concomitantly inhibiting proteases and enhancing protease inhibitors. These actions favor matrix accumulation, particularly of collagen and fibronectin (FN) implicated in progressive tissue fibrosis.[9,10] In *in vitro* standard monolayer cell culture, it has been observed that myofibroblast transdifferentiation can be induced by TGF-β1 with a concomitant expression of alpha smooth muscle actin (α-SMA).[11,12] Few studies have examined whether or not three-dimensional (3D) culture conditions affect TGF-β1 regulation and whether measured responsiveness to the 3D environment differs from the two-dimensional (2D) environment. Previous studies have demonstrated that the 3D culture system influences the cell phenotype and function, gene expression profiles and responsiveness to exogenous signals, differently from the 2D culture system.[13,14]

A common hydrogel utilized for 3D cell culture is a hyaluronan (HA)-based scaffold—Carbylan GSX (Glycosan, Salt Lake City, UT). Previous studies have shown Carbylan-GSX is biocompatible and nontoxic to fibroblasts, and it enhances overall healing and tissue regeneration in *in vitro* 2D environment and in *in vivo* animal models.[14–17] HA is a ubiquitous connective tissue glycosaminoglycan that is a vital element of the ECM, providing tissues with an optimal environment for cell attachment,[14,18] migration, and growth.[15] In addition, HA is an important mediator of the inflammatory cascade, not only recruiting immune cells to the site of wounded tissue, but contributing to granulation tissue formation,[15] amplifying the normal wound-healing response, and promoting tissue regeneration.[15,17] HA has been found to mediate cellular responses to TGF-β1 inducing fibroblast to myofibroblast differentiation[19] and altering TGF-β1-dependent proliferation in 2D culture.[20] Consequences of *in vitro* 3D HA culture on the cellular responses to TGF-β1

Division of Otolaryngology–Head and Neck Surgery, Department of Surgery, University of Wisconsin Madison, Madison, Wisconsin.

and whether these responses differ from 2D HA culture has yet to be elucidated. In the present study, we hypothesize that the presence of exogenous HA will regulate the fibroblastic response to TGF-β1. In particular, we expect that culture conditions (2D vs. 3D) will differentially affect cell morphology, proliferation, TGF-β1-induced fibroblast to myofibroblast transition as well as the extent of ECM regulation and remodeling.

Materials and Methods

Hydrogel preparation

Injectable chemically modified HA-gelatin hydrogel (Carbylan-GSX) was synthesized using a biocompatible, thiol-modified semisynthetic glycosaminoglycan (HA-DTPH), thio-modified gelatin (gelatin-DTPH), and crosslinked by a poly(ethylene glycol) diacrylate, where the final gelatin concentration was 5% (w/v). Detailed explanations of the procedures and hydrogel formulations have been described previously.[14,21–24] Carbylan-GSX gelation occurred within 10 min at 37°C.

2D and 3D culture

Normal human vocal fold fibroblasts (hVFF) were isolated from a 21-year-old donor and cultured as previously described.[25] Briefly, surgically resected vocal fold lamina propria tissue was cut into small pieces and suspended in the Dulbecco's Modified Eagle's medium supplemented with 10% fetal bovine serum (FBS), 100 U/mL penicillin, 0.01 mg/mL streptomycin sulfate, and 1×NEAA (all from Sigma, St. Louis, MO). After 14 days, the adherent confluent hVFF were trypsinized and passed. After two passaging, all cells were considered fibroblasts using standard morphological and immunocytochemical criteria.[26] Purified hVFF were steadily transfected with the retroviral vector plasmid DNA encoding human telomerase reverse transcriptase, and immortalized cells were shown to have similar morphological features and ECM gene expression past passage 25 compared to primary cells.[27] In the present study, we used immortalized cells between passages 3 and 12. Quiescent cells were obtained by briefly washing (twice) proliferating cells in the Earle's balanced salt solution, and thereafter incubating them in a medium supplemented with 0.1% Bovine Serum Albumin (BSA) for 24 h.[28]

For 3D culture, 500 μL of Carbylan-GSX and cells (2×10^6 cells/mL) were placed onto transwell permeable supports (inserts with 0.4-μm membrane pore size; Millipore Inc. Billerica, MA) in six-well plates and after a gelatin (gel thickness was approximately 0.5 mm) cell culture medium (DMEM-10% FBS) was added above and below the gel. Cells (1.6×10^5/well) grown on Carbylan-GSX surface (2D) and standard tissue culture polystyrene surface (TCP) were controls. Cell concentration was calculated such that a cell concentration of 1×10^6 cells/mL in 3D is equivalent to a plating density of 1×10^4 cells/cm^2 with respect to maintenance of constant cell-to-cell distance.[29,30] To characterize the cellular response to TGF-β1, cells were treated with various dosages of recombinant TGF-β1 (0.1, 1, 5, 10, and 20 ng/mL; Sigma) in DMEM-0.1% BSA medium for 24 to 72 h after 24-h cell starvation.

Immunocytochemistry staining

After 48 h of 5 ng/mL TGF-β1 treatment, primary antibodies at the appropriate dilution in 10% normal goat serum in phosphate-buffered saline (PBS) were applied for 90 min to cells grown in Carbylan-GSX (3DHA), on Carbylan-GSX (2DHA) and TCP slide chambers. Antibodies included hPH (collagen biosynthase; Millipore, Billerica, MA), α-SMA (myofibroblast marker; Sigma), type I and type II TGF-β1 receptor (TGFBRI and TGFBRII; Abcam, Cambridge, MA). Appropriate secondary antibodies (Alexa goat anti-mouse 488; or Alexa goat anti-rabbit 568; Invitrogen, Carlsbad, CA) diluted in PBS at 1:200 were applied for 60 min at room temperature. After mounting with Vector aqueous anti-fade fluorescent mounting medium containing 4',6-diamidino-2-phenylindole, slides were imaged by a high-speed spectral confocal laser microscope (Nikon A1R). The primary antibody was omitted for the negative control.

Western blot analysis

To examine the effect of TGF-β1 on fibroblast differentiation in Carbylan-GSX, Western blot assay was performed using antibodies specific to α-SMA and GAPDH (Sigma). Total cellular proteins were extracted using M-PER reagent (Pierce, Rockford, IL) from cells after 48 h treatment of TGF-β1, three μg of total protein extract was separated by electrophoresis on 10% NuPAGE Bis-Tris gels using GAPDH as a loading control. Proteins were electro-transferred onto PVDF membrane (Invitrogen), and membranes were then blocked overnight in 5% skim milk at 4°C. Individual membranes were incubated in the PBS-T buffer containing anti-human antibodies against α-SMA and GAPDH followed by 30-min incubation with a secondary antibody conjugated to alkaline phosphatase (Invitrogen). Blots were developed using the Novex alkaline phosphatase chemiluminescence substrate (Invitrogen).

Cell proliferation assay

Cell proliferation for TCP, 2DHA, and 3DHA was determined using the CellTiter-Glo Luminescent Cell Viability Assay (Promega, Madison, WI) as described previously.[14] For 3D, briefly, a volume of 75 μL of the cell–gel mixture at the concentration of 2×10^3 cells/well was dispensed into each well of a 96-well plate and allowed to solidify at 37°C for 10 min; a complete medium (75 μL) containing FBS was then added to each well. Controls were monolayer cells grown on TCP and 2D HA. Cells were incubated with various dosages of TGF-β1 (0.1 to 20 ng/mL) for 72 h following 24 h starving in the DMEM-0.1% BSA. Cell numbers in quadruplicate were monitored by ATP levels (Relative Luminescent Unit) released from live cells.[31–33]

Matrix metalloproteinase activity

Matrix metalloproteinase 1 (MMP1) and MMP2 activities were determined using casein and gelatin zymograms. After 48 h treatment with TGF-β1, cell culture media from TCP, 2DHA, and 3DHA were collected and concentrated using a centrifugal concentrator (Millipore, Inc. Billerica, MA). Five to ten μl of the concentrated media with a loading buffer were electrophoretically separated in 12% casein and 10% gelatin gels (Invitrogen) at 125V for 2 h in the Tris-Glycine

sodium dodecyl sulfate Running Buffer. After electrophoresis, gels were incubated in a renaturation buffer (Invitrogen) at room temperature for 30 min, and then in a development buffer (Invitrogen) at 37°C overnight. Gels were rinsed and stained with 0.5% Coomassie blue in 30% methanol and 10% acetic acid. After destaining, light translucent bands over a blue background were detected for caseinolytic activity (MMP1 activity) and gelatinolytic activity (MMP2). No bands other than MMP1, proMMP2, and active MMP2 were identified on casein and gelatin zymography.

Gene expression analysis

To determine the effect of TGF-β1 on mRNA expression of collagen I α-2 (Col1), collagen III α-1 (Col3), FN, α-SMA, MMP1, MMP2, TIMP3, TGFBRI, and TGFBRII genes, quantitative real-time polymerase chain reaction (qPCR) was conducted. Total RNA was extracted from the cells in and on Carbylan-GSX and TCP after 24 h treatment with various doses of TGF-β1. Reverse transcription (RT) and qPCR (standard curve method) were performed as described elsewhere.[14,34] Briefly, PCR reactions for each target gene (Table 1) were conducted using a LightCycler 1.5 System (Roche, Indianapolis, IN). Target gene expression (ng/μL) was normalized by a housekeeping gene, β-Actin (ng/μL), and used to determine quantitative alterations in mRNA levels. To confirm amplification of specific transcripts, melting curve profiles were developed at the end of each PCR by cooling the sample to 40°C, and then heating it slowly to 95°C while continuously measuring the fluorescence. Every sample was tested in triplicate. Ratios of MMP to TIMP3 mRNA levels were calculated by β-Actin normalized MMPs over β-Actin normalized TIMP3.

Statistical analysis

All experiments were performed at least three times. Results of cell proliferation and gene expression were expressed as mean ± standard deviations (SD) of triplicate or quadruplicate assays. Multiple comparisons were performed for cell proliferation and gene expression by using Fisher's protected least significant difference tests. A p-value less than 0.05 was considered statistically significant. All analyses were performed using SAS statistical software version 9.1 (SAS Institute Inc., Cary, NC).

Results

Cell proliferation

Cell proliferation rates in response to TGF-β1 were judged by the amount of ATP released from proliferating cells using the CellTiter-Glo Luminescent Cell Viability Assay. Cell proliferation assay results (ATP RLU) are expressed as mean ± SD for quadruplicated samples per condition. After 72 h incubation, all concentrations of TGF-β1 (0.1 to 20 ng/mL) significantly induced hVFF proliferation on TCP and HA (2D) (Fig. 1A, B, $p < 0.01$) in a dose-dependent manner. TGF-β1 (1, 5, 10 ng/mL) produced maximal stimulation of hVFF proliferation. However, in 3DHA, it was noted that basal hVFF proliferation rates were lower than TCP and 2D HA. In 3D HA, TGF-β1 (0.1, 1, and 5 ng/mL) caused an insignificant increase in cell proliferation (Fig. 1C, $p > 0.05$).

Table 1. Primer Sequences and Products of Reverse Transcription–Polymerase Chain Reaction

| Gene	Genebank#	Forward primer	Reverse primer	Size
α-SMA	NM_001141945	5'-CCAGCAGATGTGGATCAGCAAACA-3'	5'-ACGAGTCAGAGCTTTGGCTAGGAA-3'	179 bp
Collagen I α-2	NM_000089	5'-AACAAATAAGCCATCACGCCTGCC-3'	5'-TGAAACAGACTGGGCCAATGTCCA-3'	101 bp
Collagen III α-1	NM_000090	5'-CCATTGCTGGGATTGGAGGTGAAA-3'	5'-TTCAGGTCTCTGCAGTTTCTAGCGG-3'	187 bp
Fibronectin	NM_002026	5'-ACCTACGGATGACTCGTGCTTTGA-3'	5'-CAAAGCCTAAGCACTGGCACAACA-3'	116 bp
MMP1	NM_002421	5'-TGCAACTCTGACGTTGATCCCAGA-3'	5'-ACTGCACATGTGTTCTTGAGCTGC-3'	122 bp
MMP2	NM_004530	5'-AGAAGGATGGCAAGTACGGCT-3'	5'-AGTGGTGCAGCTGTCATAGGATGT-3'	128 bp
TIMP3	NM_000362	5'-TGATGCAGCACACAAATTCCC-3'	5'-AAGCTCTGTTATTCTGGCCTGGGT-3'	102 bp
TGFBRI	NM_004612	5'-TCAGTGCACCCTTGTTACTTGGGA-3'	5'-AAGCCCTGCAGAGACTTCATAGCA-3'	188 bp
TGFBRII	NM_001024847	5'-AGTGTGGGTGGGCTGAGAGTTAAA-3'	5'-ACCACTAGAGGTCAATGGGCAAACA-3'	127 bp
β-Actin	NM_001101	5'-ACGTTGCTATCCAGGCTGTGCTAT-3'	5'-CTCGGTGAGGGATCTTCATGAGGTAGT-3'	188 bp
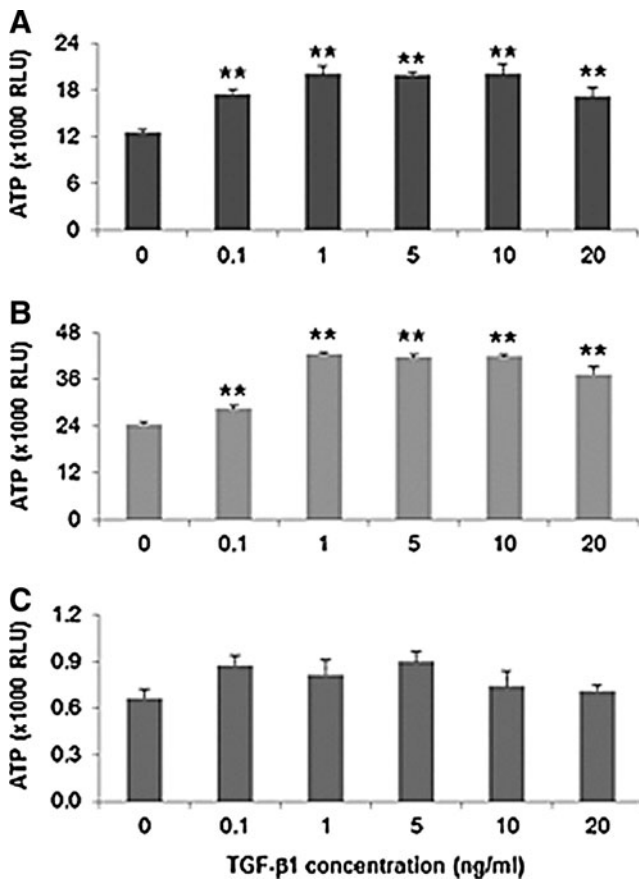
FIG. 1. Proliferation effect of transforming growth factor–β1 (TGF-β1) on cells plated on tissue culture polystyrene (TCP) **(A)**, on Carbylan-GSX **(B)**, and in three-dimensional (3D) Carbylan-GSX **(C)** at 2000 cells/well of a 96-well plate. After 24 h starvation, cells were treated with various doses (0.1 to 20 ng/mL) of TGF-β1 for 72 h. Cell numbers in quadruplicate were monitored by ATP levels (RLU). **$p < 0.01$.

Cell morphology and differentiation

To compare the effects of TGF–β1 on cell morphology, we cultured fibroblasts in three conditions—on TCP, on HA (2D), and in HA (3D). Under resting, serum-free unstimulated conditions, cells on TCP and HA (2D) displayed a typical large spindle shaped appearance (Fig. 2A, B); cells in 3D HA were smaller and round in appearance (Fig. 2C).

To characterize differentiation of a myofibroblast phenotype on 2D HA and in 3D HA, after 48 h treatment with 5 ng/mL recombinant TGF-β1, cells were detected by immunocytochemistry staining and compared to untreated controls (Fig. 2). On TCP, cells were larger and polygonal with obvious α-SMA deposition identifying cytoplasmic myofilaments along the cell axis (Fig. 2D); cells on 2D HA showed similar morphology as TCP, but with weaker and less α-SMA staining (Fig. 2E). Cells grown in 3D HA remained round and small compared to controls with modest α-SMA staining (Fig. 2F). This experiment was repeated more than three times with consistent results.

Our morphological results were corroborated by using qPCR and Western blot assays. On TCP, α-SMA mRNA expression (Fig. 3A) was significantly upregulated by TGF-β1 ($p < 0.0001$) compared to 2D HA and 3D HA. However, in 2D

HA and 3D HA culture, *α-SMA* mRNA expression levels were significantly downregulated by TGF-β1 ($p < 0.0001$). For protein expression levels, TCP conditions had low levels of α-SMA expressed in quiescent cells and after incubating with TGF-β1, α-SMA protein expression was markedly increased. When treating with 5 and 10 ng/mL TGF-β1, the α-SMA protein reached maximum levels. Five ng/mL TGF-β1 was chosen for further study. However, with similar total protein loading, α-SMA protein expression was not detected for cells in 2D HA and 3DHA environments even after TGF-β1 stimulation (Fig. 3B).

ECM regulation

To determine whether ECM expression of fibroblasts was altered by the presence of HA, mRNA expression of collagen I α-2 (*Col1*), collagen III α-1 (*Col3*), and *FN* were measured by the qPCR assay (Fig. 4). Before TGF-β1 stimulation, expression of *Col1*, *Col3*, and *FN* was significantly decreased in 2D HA and 3D HA conditions compared to TCP and this decrease was more marked in 3D HA versus 2DHA. After TGF-β1 treatment, *Col1* expression was significantly downregulated in TCP and 2D HA ($p < 0.0001$), and in 3D HA it was consistently at a lower level. *Col3* expression was also significantly downregulated by TGF-β1 in TCP and both HA conditions ($p < 0.0001$). *FN* gene expression was downregulated by TGF-β1 in TCP across all treatment levels ($p < 0.0001$), except for 0.1 ng/mL. *FN* expression for both HA conditions remained stable across all treatment levels, except for 3D HA at 10 and 20 ng/mL of TGF-β1, where significant increases were observed ($p < 0.0001$, respectively).

For analysis of ECM degradation, measurements of MMP1 and MMP2 were made utilizing zymogram, where bands representing MMP1, latent, and active forms of MMP2 activities were observed (Fig. 5). MMP1 (52 kDa) was higher in 3D HA than TCP and 2D HA (Fig. 5A). Intense banding for the active form of MMP2 (65 kDa) was detected for 3D HA (Fig. 5B). For pro-MMP2 (72 kDa), no significant differences were observed for the three conditions. Both MMP1 and the active form of MMP2 were enhanced in 3D HA, suggesting that hVFF cultured in 3D HA could produce more MMP1 and MMP2 for degrading and remodeling ECM. There were no significant differences for MMP1 and MMP2 activities with various TGF-β1 dosages.

To further confirm our zymograph results, we analyzed mRNA levels of *MMPs*, *TIMP3*, and their ratios with qPCR. The presence of HA (2D and 3D) significantly upregulated *MMP1* and downregulated *TIMP3* mRNA expression ($p < 0.0001$, Fig. 6) with a greater effect for 3D HA than 2D HA (*p* values, respectively <0.05 and <0.01). *MMP2* was also downregulated by HA ($p < 0.0001$), with 2D HA causing a greater decrease than 3D. Subsequently, these outcomes produced significantly high ratios of *MMP1* to *TIMP3* in 2D HA (7.3-fold compared to TCP, $p < 0.0001$) and 3D HA (14.9-fold compared to TCP, $p < 0.0001$). In 3D HA, the *MMP2/TIMP3* ratio was significantly increased 2.3-fold over TCP and 2D HA ($p < 0.0001$). Furthermore, TGF-β1 significantly downregulated *MMP1*, *MMP2*, and *TIMP3* expression across all culture conditions (TCP, 2D HA, and 3D HA) in a dose-dependent manner ($p < 0.0001$), except for *MMP2* in 3D HA, which remained consistently at higher levels compared to control ($p < 0.0001$). Consequently, after TGF-β1 (0.1 to
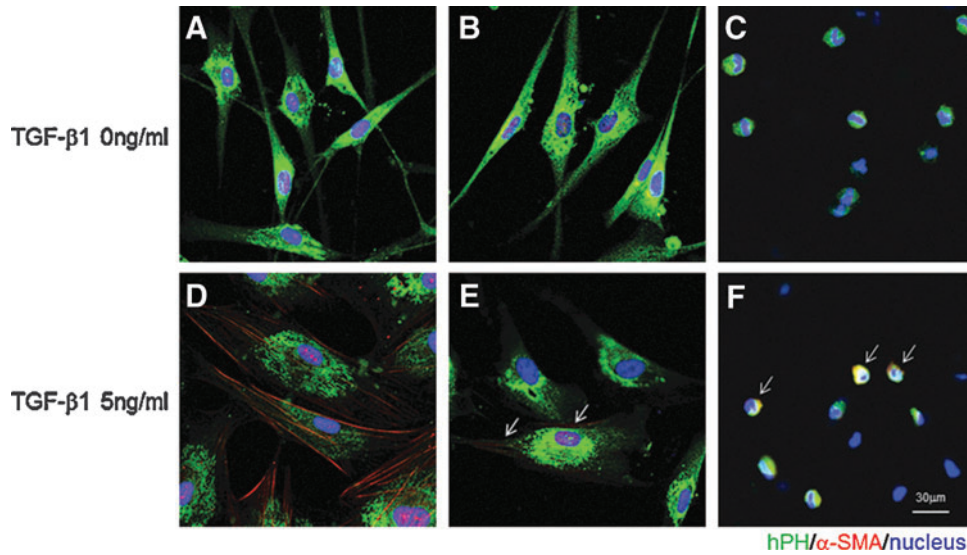
FIG. 2. Representative images of human vocal fold fibroblasts (hVFF) on TCP, two-dimensional (2D) hyaluronan (HA), and in 3D HA in response to TGF-β1 by hPH/alpha smooth muscle actin (α-SMA) double-immunofluorescence analysis. Morphological analysis of hVFF cultured on the TCP surface without TGF-β1 showed a typical spindle shape **(A)** and on the surface of HA cells showed the similar shape **(B)**. However, hVFF were of smaller rounded morphology in 3D HA **(C)**. Double-immunostaining of the cells with 5 ng/mL TGF-β1 treatment demonstrated strong expression of α-SMA along cell axis on the TCP surface **(D, red)**, low expression on HA **(E)** and in HA **(F, red as arrow)**. Nuclei were counter-stained with 4′,6-diamidino-2-phenylindole (DAPI). Scale bar: 60 μm.
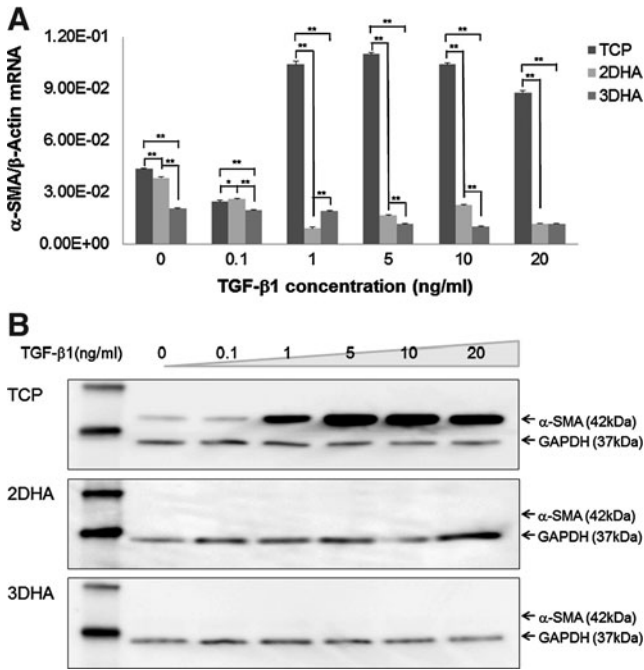

FIG. 3. Quantitative real-time polymerase chain reaction (qPCR) and Western blot analyses of α-SMA expression in the hVFF. Cells grown on TCP, 2D HA, and in 3D HA were treated with various doses of TGF-β1. After 24 h, α-*SMA* mRNA levels were analyzed by qPCR **(A)**. Data are expressed as mRNA expression for the α-*SMA* gene (ng/μL) relative to *β-Actin* (ng/μL). Values represent mean ± SD of triplicated assays. *$p < 0.05$; **$p < 0.01$. After 48 h of TGF-β1 treatment, quantification of α-SMA protein levels of whole-cell lysates were analyzed by Western blot analysis **(B)**. The first lane (MW) was the protein ladder. GAPDH (37 kDa) was used to demonstrate equal loads of total protein amount in different lanes.
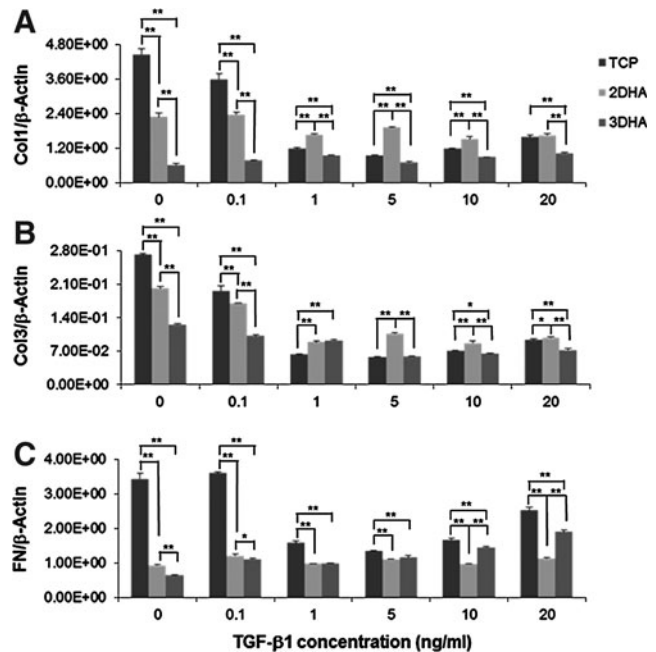

FIG. 4. Effect of TGF-β1 on the gene expression of ECM components. hVFF on TCP, 2D HA, and in 3D HA were treated with various doses of TGF-β1 for 24 h, and were subjected to qPCR. Data are expressed as mRNA expression for Collagen I (*Col1*), III (*Col3*), and fibronectin (*FN*) gene (ng/μL) relative to *β-Actin* (ng/μL). Values represent mean ± SD of triplicated assays. *$p < 0.05$; **$p < 0.01$. **(A)** TGF-β1-inducible *Col1* mRNA levels. **(B)** TGF-β1-inducible *Col3* mRNA levels. **(C)** TGF-β1-inducible *FN* mRNA levels.
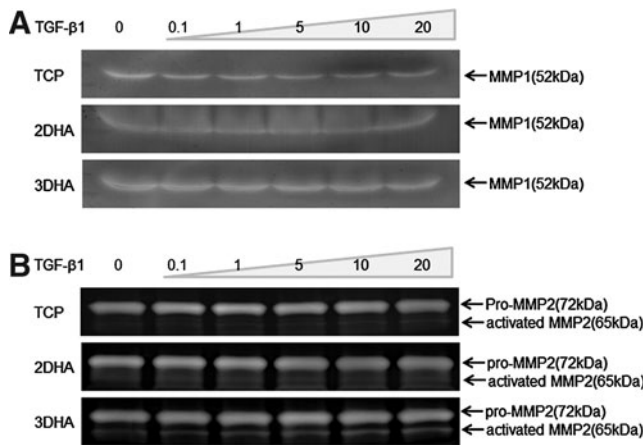
FIG. 5. Regulation of matrix metalloproteinase (MMP1 and MMP2) activity by culture condition. hVFF grown on TCP, 2D HA, and 3D HA were starved for 24 h before the addition of various doses of TGF-β1 for 48 h. Equal amounts of cell supernatant were analyzed by the Zymogram assay. **(A)** MMP1 activity assay was performed by casein zymogram. **(B)** MMP2 activities were assayed by gelatin zymogram.

20 ng/mL) treatment, significantly high ratios of MMP1 to TIMP3 and MMP2 to TIMP3 were observed in 2D HA and 3D HA compared to TCP (Fig. 6D, E, $p < 0.0001$).

Expression of TGF-β receptors

To further search the mechanism of TGF-β1-induced hVFF function change on or in HA, the expression of type I and type II TGF-β receptors (*TGFBRI* and *TGFBRII*) were analyzed in hVFF using qPCR and immunocytochemistry, particularly after TGF-β1 stimulation. Gene expression of *TGFBRI* was significantly upregulated in 2D HA and 3D HA conditions compared to TCP ($p < 0.0001$), and in 3DHA it was significantly increased after treatment of TGF-β1 in a dose-dependent manner ($p < 0.0001$, Fig. 7A). Although *TGFBRII* gene expression was downregulated by TGF-β1 in these three conditions, its expression levels were significantly higher in both HA conditions than TCP ($p < 0.0001$, Fig. 7B). Thereby, the presence of HA (both 2D and 3D) led to the significant increase of *TGFBRI* and *TGFBRII* gene expression, chiefly after TGF-β1 treatment. However, the expression patterns of TGFBRI and TGFBRII (Fig. 8A, B) were similar in TCP, 2D HA, and 3D HA conditions with or without TGF-β1 treatment, although their cell sizes were judged to be different (cells were enlarged in the presence of 5 ng/mL TGF-β1).

Discussion

During recent years, it has become increasingly clear that cells are not only influenced by biochemical cues, but also by physical aspects, such as stiffness and geometry of the extracellular environment. These physical parameters have a major impact on cell fate and function, with dramatic consequences for tissue function. Most of our current knowledge on cell behavior and differentiation is derived primarily from studies on rigid and planar 2D tissue culture substrates that are homogeneously coated with biomolecules. There is an increasing demand for *in vitro* models that capture more of the relevant complexity present in 3D models. In this in-
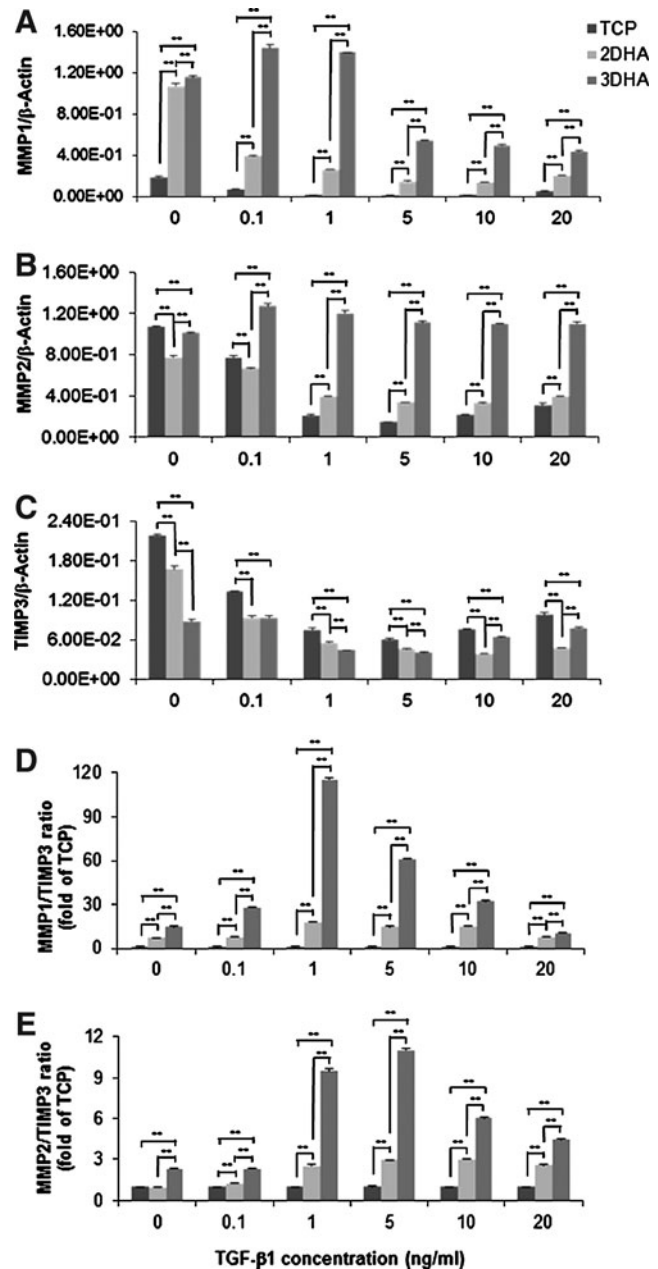

FIG. 6. Effect of TGF-β1 on *MMP1*, *MMP2*, and *TIMP3* mRNA expression. hVFF seeded on TCP, 2D HA, and 3D HA were treated with various doses of TGF-β1 for 24 h, and were subjected to qPCR. Data are expressed as mRNA expression for *MMP1*, *MMP2*, and *TIMP3* (ng/μL) relative to β-Actin (ng/μL). The ratios of *MMPs* to *TIMP3* were calculated by β-Actin normalized *MMPs* over β-Actin normalized *TIMP3*. Values represent mean±SD of triplicated assays. **$p < 0.01$. **(A)** TGF-β1-inducible *MMP1* mRNA levels; **(B)** TGF-β1-inducible *MMP2* mRNA levels; **(C)** TGF-β1-inducible *TIMP3* mRNA levels; **(D)** ratios of *MMP1* expression to *TIMP3*; **(E)** ratios of *MMP2* expression to *TIMP3*.

vestigation, we used a HA hydrogel to create a 3D cell culture environment to study the influence on the behavior of hVFF and their response to the cytokine, TGF-β1. Using this 3D model, hVFF were shown to be smaller and rounded in morphology, which is clearly different with the elongated, spindle morphology seen in 2D conditions (i.e., HA
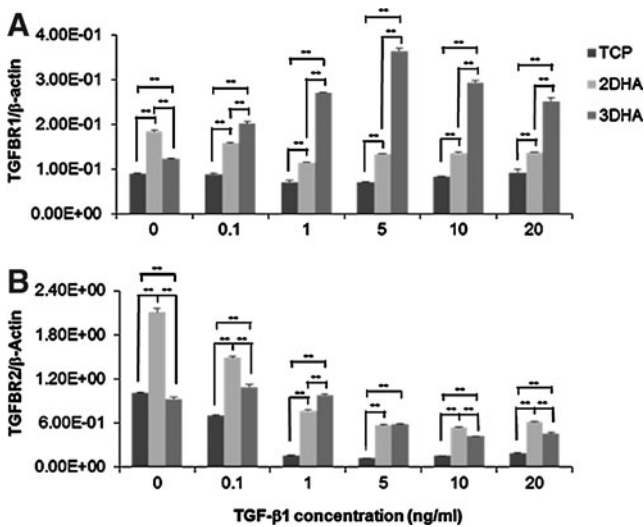
FIG. 7. Effect of TGF-β1 on the mRNA expression of TGF-β receptors. hVFF seeded on TCP, 2D HA, and in 3D HA were treated with various doses of TGF-β1 for 24 h, and were subjected to qPCR. Data are expressed as mRNA expression for type I (*TGFBRI*) and type II (*TGFBRII*) of TGF-β receptor (ng/μL) relative to β-Actin (ng/μL). Values represent mean±SD of triplicated assays. **$p < 0.01$. **(A)** TGF-β1-inducible *TGFBRI* mRNA levels. **(B)** TGF-β1-inducible *TGFBRII* mRNA levels.

hydrogel, TCP, collagen, and Matrigel).[14] This smaller, rounded morphology phenomenon was been observed with other 3D environments, including Matrigel,[13,14] collagen,[35,36] and PEG-L-PA thermogel [a poly-(ethylene glycol)-b-poly (L-alanina) gel].[37] Investigations by Kumar and others[38–40] used different features of the extracellular environment to observe changes in cell morphology and related cell behaviors. They found that the cell shape could be influenced by matrix structure, stiffness, and molecular components.

The matrix structure influences the cell shape by physical forces,[38,40] while matrix molecules could control the cell shape by adjusting the distribution of cell–substrate contact sites.[39,40] In our 3D experiments,[14] we found that near the top surface of a HA gel or Matrigel, hVFF would spread out to a flatten spindle shape (data were not shown), suggesting that in 3D hVFF, the smaller and rounded morphology is caused by the matrix structure–physical force. It has been reported that cell behavior and function are related to their morphological features.[38,39,41,42] Glowacki *et al.* suggested that the cell shape is an important factor for chondrocyte function. These studies demonstrated that cells held in the rounded phenotype proliferated slowly, incorporated low levels of thymidine into DNA, and integrated large amounts of sulfate into glycosaminoglycans,[39] while chondrocytes that retained a fibroblast-like shape were flattened, showed more rapid growth, greater thymidine incorporation, and lower sulfate uptake. It was concluded that the cell shape played an important role in phenotypic expression and behaviors. Other experiments by Folkman and Moscona using bovine aortic endothelial cells showed similar findings in that as cells were modified from the flatten to spheroid shape, cell proliferation decreased.[43] Kumar *et al.* has demonstrated that the differentiation of human bone

marrow stromal cells to osteogenic lineage is also mediated by the cell shape.[38] Clearly, cell morphology and cell function are strongly linked;[43,44] however, the relevant underlying mechanism remain unclear.

Biomaterial stiffness is also very important for cell proliferation and behavior.[45] Increased stiffness of a matrix (PEG gels) has been demonstrated to act as a physical barrier for cells in 3D, impeding their proliferation and migration,[45] Except of cell shape and matrix stiffness, Schor suggested that the cell proliferation rate in 3D depended on the cell types.[36] In our previous work, we compared the proliferation and function of vocal fold fibroblasts on TCP, 2D and 3D of HA hydrogel and Matrigel,[14] demonstrating that in 3D HA, smaller, rounded fibroblasts proliferated at lower rates and expressed less collagen I RNA compared to TCP and 2D HA. Similar results were found with a 3D Matrigel condition. In the current study, we examined the effect of TGF-β1 on hVFF proliferation in 3D HA. We found that TGF-β1 enhanced hVFF proliferation rates—cell proliferation was greater when cells were grown on TCP and 2D HA and less proliferative when grown in 3D HA. Similar responses to TGF-β1 have been observed in airway smooth muscle cells[46] and renal fibroblasts.[47] As per previous reports, the effect of TGF-β1 on cell proliferation is complex, depending on the cell type and conditions.[48–50] Our results suggest that the cell shape may play an important role in hVFF proliferation and function with significant clinical significance—application of an HA hydrogel into the wound bed may limit tissue fibrosis, which would be expected to be secondary to increased cell proliferation and excessive matrix production in the presence of resident early elevated TGF-β1.

Except for cell proliferation and excessive matrix deposition, fibroblast to myofibroblast differentiation is also widely thought to be a critical event in the pathogenesis of human fibrotic diseases via increased matrix synthesis and contraction of the tissue.[51–53] Myofibroblasts are characterized by α-SMA expression and the formation of α-SMA-containing stress fibers.[51–56] TGF-β1 can induce fibroblast-to-myofibroblast differentiation.[12,57–59] In 2008, Wells and Discher determined that the matrix stiffness was related with TGF-β1-induced myofibroblast differentiation,[60] in which they showed that higher tension could increase the release of active TGF-β1, resulting in myofibroblast differentiation. In the present study, we observed that TGF-β1 induced myofibroblast differentiation in standard monolayer culture condition at both the gene and protein levels. In the presence of HA, both 2D and 3D, we did not observe myofibroblast differentiation by the Western blot assay, suggesting that some molecules of the HA hydrogel could inhibit TGF-β1-induced myofibroblast differentiation instead of the matrix stiffness. These results are consistent with Meran's previous work, which demonstrated that 2D HA mediated the cellular response to TGF-β1, inducing fibroblast to myofibroblast differentiation,[19] indicating that 3D culture did not induce a different response.

During the *in vivo* wound-healing process, fibrogenesis, myofibroblast differentiation, cell proliferation, and excess ECM deposition occur in parallel.[61] Abnormal accumulation of various ECM proteins is paramount for fibrosis formation.[55,56] For various etiologies of injury and subsequent repair, abnormal deposition of collagen is thought to have a dual effect as excessive matrix deposition leads to fibrosis,
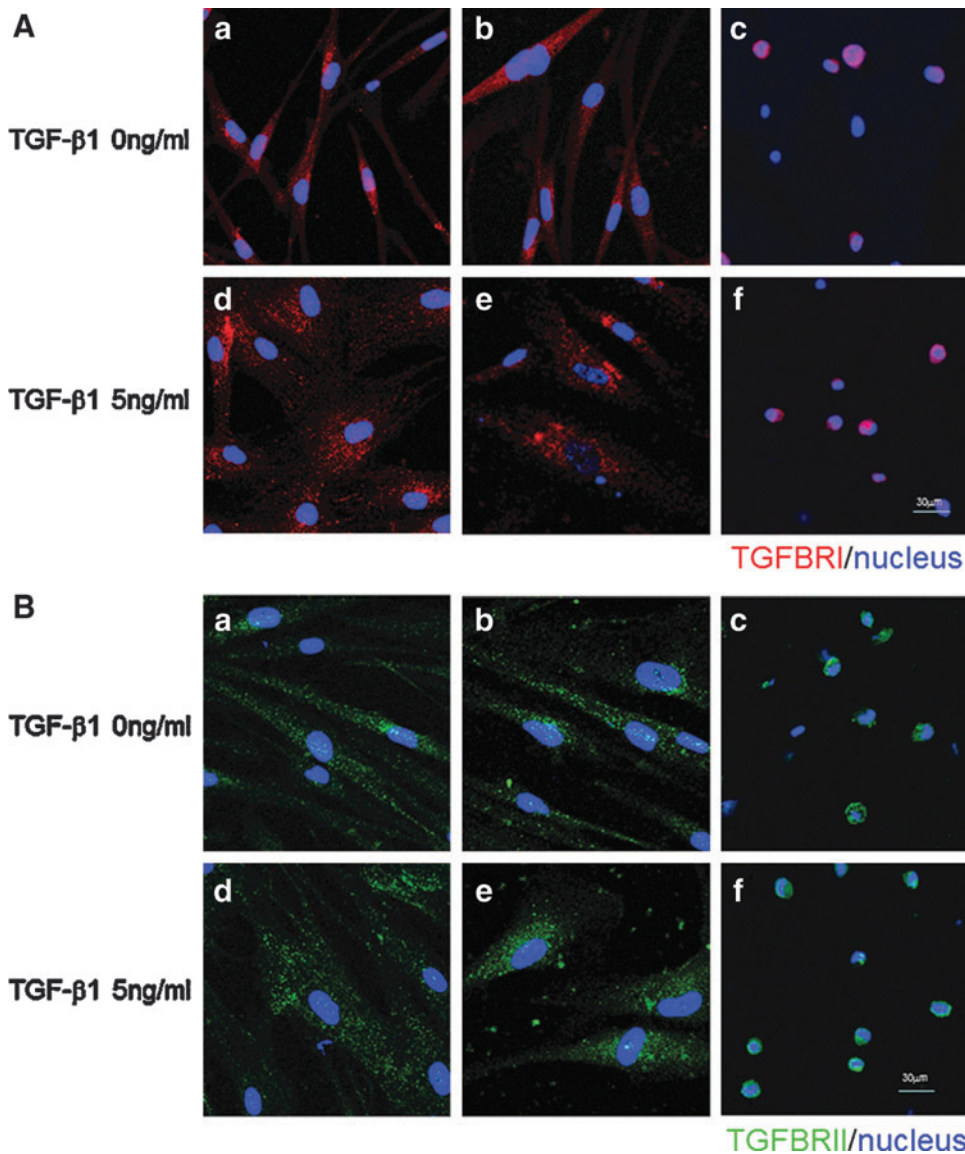
FIG. 8. Expression of TGF-β receptors in hVFF were detected by immunocytochemistry staining. TGFBRI **(A,** red**)** and TGFBRII **(B,** green**)** were observed in the cells on TCP **(a, d),** 2D HA **(b, e),** and in 3D HA **(c, f)** conditions treated with either medium alone **(a, b, c)** or 5 ng/mL TGF-β1 **(d, e, f)** for 48 h. Nuclei were counter-stained with DAPI. Scale bar: 60 μm.

which in turn impairs already attenuated tissue function. Antifibrotic agents and biomaterials that target steps in collagen synthesis and degradation pathways represent promising strategies for fibrosis diseases. Collagen I, III, and FN are the main ECM components of the vocal fold lamina propria and their accumulation is the main cause of vocal fold scarring.[62–64] Regulation of ECM production and degradation could be considered a key factor in managing scarring. ECM regulation is mainly divided into two parts—synthesis and degradation. MMP1 and MMP2 are known to degrade a wide range of ECM molecules, including type I and III collagen, FN, elastin, and decorin. Although TIMP1 and TIMP2 play a key role in maintaining the balance between ECM deposition and degradation, TIMP3 is the only member of TIMP family, which is found exclusively in the ECM,[65] inhibiting MMP activity, causing excessive deposition of ECM, and resulting in tissue fibrosis. In this study, we investigated ECM regulation by analyzing ECM production and degradation in different culture environments. In 2D and 3D HA unstimulated conditions, ECM components (collagen I, III, and *FN*) were

downregulated. Notably in 3D HA, after TGF-β1 treatment, collagen I and III expression remained at a lower level compared to TCP and 2D HA. In addition, we found that 3D HA increased MMP1 and MMP2 activity, and both 2D and 3D HA significantly upregulated *MMP1* and downregulated *TIMP3* gene expression, which caused a marked increase of the ratios of *MMP1* to *TIMP3* and *MMP2* to *TIMP3*. 3D HA showed a stronger response than 2D HA (Fig. 6). Lastly, our results demonstrated that pro-MMP2 activities were similar in TCP, 2D HA, and 3D HA conditions, however, the levels of *MMP2* mRNA were different; 3D HA stimulated the transformation of pro-MMP into active MMP2. Although TGF-β1 did not increase the activities of MMP1 and MMP2, it significantly upregulated their gene expression and increased ratios of *MMP1/TIMP3* and *MMP2/TIMP3* in the 3D HA condition. In all, these results indicated that HA regulated fibroblast function through ECM synthesis, degradation, remodeling, and promotion of wound healing, and hVFF showed a more significant response in 3D HA versus the 2D HA environment.

TGF-β1 functions through binding of the extracellular domain of its type II receptor (*TGFBRII*),[66,67] transphosporylating the type I receptor (*TGFBRI*), activating its kinase, and initiating downstream signaling. The inhibition or modification of this pathway has been considered a promising therapeutic strategy to inhibit tissue fibrosis.[68] In the present study, it was found that the cellular response to TGF-β1 was reduced or inhibited in the presence of HA, while the gene expression of TGFBRI and TGFBRII were significantly upregulated, the 3D environment to a greater extent than 2D, although their distribution patterns were similar. This phenomenon suggests that exogenous HA molecules might act downstream of the TGF-β1 signaling pathway through its receptors. Further investigation of this phenomenon is warranted.

Conclusions

We have shown that *in vitro* 2D HA and 3D HA culture of hVFF can suppress ECM production, enhance ECM degradation and remodeling, and inhibit myofibroblast differentiation in response to TGF-β1, compared to standard TCP culture. 3D HA modulated greater TGF-β1 consequences than 2D HA on the aforementioned processes without a decrease in TGF-β receptor expression. We speculate that 3D HA regulates cell function though a downstream pathway of TGF-β1. Additionally, this study suggests that exogenous HA could facilitate a decreased fibrotic response, improve wound healing and prevent scar formation even in the presence of TGF-β1. Future investigation is necessary to determine possible regulation of TGF-β1 downstream signals by exogenous HA.

Acknowledgments

Disclosure Statement

No competing financial interests exist.

References

1. Clark, R.A. Biology of dermal wound repair. Dermatol Clin **11,** 647, 1993.
2. Bissell, M.J., Hall, H.G., and Parry, G. How does the extracellular matrix direct gene expression? J Theor Biol **99,** 31, 1982.
3. Schachtrup, C., Ryu, J.K., Helmrick, M.J., Vagena, E., Galanakis, D.K., Degen, J.L., *et al.* Fibrinogen triggers astrocyte scar formation by promoting the availability of active TGF-beta after vascular damage. J Neurosci **30,** 5843, 2010.
4. Tandon, A., Tovey, J.C., Sharma, A., Gupta, R., and Mohan, R.R. Role of transforming growth factor Beta in corneal function, biology and pathology. Curr Mol Med **10,** 565, 2010.
5. Grande, J.P. Role of transforming growth factor-beta in tissue injury and repair. Proc Soc Exp Biol Med **214,** 27, 1997.
6. Massaous, J., and Hata, A. TGF-beta signalling through the Smad pathway. Trends Cell Biol **7,** 187, 1997.
7. Sporn, M.B., and Roberts, A.B. Transforming growth factor-beta: recent progress and new challenges. J Cell Biol **119,** 1017, 1992.
8. Rifkin, D.B., Kojima, S., Abe, M., and Harpel, J.G. TGF-beta: structure, function, and formation. Thromb Haemost **70,** 177, 1993.
9. Branton, M.H., and Kopp, J.B. TGF-beta and fibrosis. Microbes Infect **1,** 1349, 1999.
10. Border, W.A., and Noble, N.A. Transforming growth factor beta in tissue fibrosis. N Engl J Med **331,** 1286, 1994.
11. Krummel, T.M., Michna, B.A., Thomas, B.L., Sporn, M.B., Nelson, J.M., Salzberg, A.M., *et al.* Transforming growth factor beta (TGF-beta) induces fibrosis in a fetal wound model. J Pediatr Surg **23,** 647, 1988.
12. Vyas, B., Ishikawa, K., Duflo, S., Chen, X., and Thibeault, S.L. Inhibitory effects of hepatocyte growth factor and interleukin-6 on transforming growth factor-beta1 mediated vocal fold fibroblast-myofibroblast differentiation. Ann Otol Rhinol Laryngol **119,** 350, 2010.
13. Kraehenbuehl, T.P., Zammaretti, P., Van der Vlies, A.J., Schoenmakers, R.G., Lutolf, M.P., Jaconi, M.E., *et al.* Three-dimensional extracellular matrix-directed cardioprogenitor differentiation: systematic modulation of a synthetic cell-responsive PEG-hydrogel. Biomaterials **29,** 2757, 2008.
14. Chen, X., and Thibeault, S.L. Biocompatibility of a synthetic extracellular matrix on immortalized vocal fold fibroblasts in 3-D culture. Acta Biomater **6,** 2940, 2010.
15. Duflo, S., Thibeault, S.L., Li, W., Shu, X.Z., and Prestwich, G. Effect of a synthetic extracellular matrix on vocal fold lamina propria gene expression in early wound healing. Tissue Eng **12,** 3201, 2006.
16. Duflo, S., Thibeault, S.L., Li, W., Shu, X.Z., and Prestwich, G.D. Vocal fold tissue repair *in vivo* using a synthetic extracellular matrix. Tissue Eng **12,** 2171, 2006.
17. Thibeault, S.L., Klemuk, S.A., Chen, X., and Quinchia Johnson, B.H. In vivo engineering of the vocal fold ECM with injectable HA hydrogels-late effects on tissue repair and biomechanics in a rabbit model. J Voice **25,** 229, 2011.
18. Serban, M.A., Liu, Y., and Prestwich, G.D. Effects of extracellular matrix analogues on primary human fibroblast behavior. Acta Biomater **4,** 67, 2008.
19. Meran, S., Thomas, D., Stephens, P., Martin, J., Bowen, T., Phillips, A., *et al.* Involvement of hyaluronan in regulation of fibroblast phenotype. J Biol Chem **282,** 25687, 2007.
20. Meran, S., Luo, D.D., Simpson, R., Martin, J., Wells, A., Steadman, R., *et al.* Hyaluronan facilitates transforming growth factor-beta1-dependent proliferation via CD44 and epidermal growth factor receptor interaction. J Biol Chem **286,** 17618, 2011.
21. Shu, X.Z., Liu, Y., Luo, Y., Roberts, M.C., and Prestwich, G.D. Disulfide cross-linked hyaluronan hydrogels. Biomacromolecules **3,** 1304, 2002.
22. Shu, X.Z., Liu, Y., Palumbo, F., and Prestwich, G.D. Disulfide-crosslinked hyaluronan-gelatin hydrogel films: a covalent mimic of the extracellular matrix for *in vitro* cell growth. Biomaterials **24,** 3825, 2003.
23. Shu, X.Z., Ghosh, K., Liu, Y., Palumbo, F.S., Luo, Y., Clark, R.A., *et al.* Attachment and spreading of fibroblasts on an RGD peptide-modified injectable hyaluronan hydrogel. J Biomed Mater Res A **68,** 365, 2004.
24. Zheng Shu, X., Liu, Y., Palumbo, F.S., Luo, Y., and Prestwich, G.D. *In situ* crosslinkable hyaluronan hydrogels for tissue engineering. Biomaterials **25,** 1339, 2004.

25. Chen, X., and Thibeault, S.L. Characteristics of age-related changes in cultured human vocal fold fibroblasts. Laryngoscope **118,** 1700, 2008.

26. Thibeault, S.L., Li, W., and Bartley, S. A method for identification of vocal fold lamina propria fibroblasts in culture. Otolaryngol Head Neck Surg **139,** 816, 2008.

27. Chen, X., and Thibeault, S.L. Novel isolation and biochemical characterization of immortalized fibroblasts for tissue engineering vocal fold lamina propria. Tissue Eng Part C Methods **15,** 201, 2009.

28. Zetterberg, A., and Engstrom, W. Mitogenic effect of alkaline pH on quiescent, serum-starved cells. Proc Natl Acad Sci U S A **78,** 4334, 1981.

29. Kim, M.S., Yeon, J.H., and Park, J.K. A microfluidic platform for 3-dimensional cell culture and cell-based assays. Biomed Microdevices **9,** 25, 2007.

30. Semino, C.E., Merok, J.R., Crane, G.G., Panagiotakos, G., and Zhang, S. Functional differentiation of hepatocyte-like spheroid structures from putative liver progenitor cells in three-dimensional peptide scaffolds. Differentiation **71,** 262, 2003.

31. David, L. and Smith, W.A.R. CellTiter-Glo Luminescent Cell Viability Assay: Application for Viability Studies of Cells Grown in Agarose. Cell Note Promega **17,** 16, 2007.

32. Crouch, S.P., Kozlowski, R., Slater, K.J., and Fletcher, J. The use of ATP bioluminescence as a measure of cell proliferation and cytotoxicity. J Immunol Methods **160,** 81, 1993.

33. Kangas, L., Gronroos, M., and Nieminen, A.L. Bioluminescence of cellular ATP: a new method for evaluating cytotoxic agents *in vitro.* Med Biol **62,** 338, 1984.

34. Larionov, A., Krause, A., and Miller, W. A standard curve based method for relative real time PCR data processing. BMC Bioinformatics **6,** 62, 2005.

35. Gillette, B.M., Jensen, J.A., Tang, B., Yang, G.J., Bazargan-Lari, A., Zhong, M., *et al. In situ* collagen assembly for integrating microfabricated three-dimensional cell-seeded matrices. Nat Mater **7,** 636, 2008.

36. Schor, S.L. Cell proliferation and migration on collagen substrata *in vitro.* J Cell Sci **41,** 159, 1980.

37. Yun, E.J., Yon, B., Joo, M.K., and Jeong, B. Cell therapy for skin wound using fibroblast encapsulated poly(ethylene glycol)-poly(l-alanine) thermogel. Biomacromolecules **13,** 1106, 2012.

38. Kumar, G., Tison, C.K., Chatterjee, K., Pine, P.S., McDaniel, J.H., Salit, M.L., *et al.* The determination of stem cell fate by 3D scaffold structures through the control of cell shape. Biomaterials **32,** 9188, 2011.

39. Glowacki, J., Trepman, E., and Folkman, J. Cell shape and phenotypic expression in chondrocytes. Proc Soc Exp Biol Med **172,** 93, 1983.

40. Klein, F., Richter, B., Striebel, T., Franz, C.M., von Freymann, G., Wegener, M., *et al.* Two-component polymer scaffolds for controlled three-dimensional cell culture. Adv Mater **23,** 1341, 2011.

41. Gruber, H.E., and Hanley, E.N., Jr. Human disc cells in monolayer vs 3D culture: cell shape, division and matrix formation. BMC Musculoskelet Disord **1,** 1, 2000.

42. Shah, J.V. Cells in tight spaces: the role of cell shape in cell function. J Cell Biol **191,** 233, 2010.

43. Folkman, J., and Moscona, A. Role of cell shape in growth control. Nature **273,** 345, 1978.

44. Chen, C.S., Mrksich, M., Huang, S., Whitesides, G.M., and Ingber, D.E. Geometric control of cell life and death. Science **276,** 1425, 1997.

45. Bott, K., Upton, Z., Schrobback, K., Ehrbar, M., Hubbell, J.A., Lutolf, M.P., *et al.* The effect of matrix characteristics on fibroblast proliferation in 3D gels. Biomaterials **31,** 8454, 2010.

46. Chen, G., and Khalil, N. TGF-beta1 increases proliferation of airway smooth muscle cells by phosphorylation of map kinases. Respir Res **7,** 2, 2006.

47. Strutz, F., Zeisberg, M., Renziehausen, A., Raschke, B., Becker, V., van Kooten, C., *et al.* TGF-beta 1 induces proliferation in human renal fibroblasts via induction of basic fibroblast growth factor (FGF-2). Kidney Int **59,** 579, 2001.

48. Moses, H.L., Yang, E.Y., and Pietenpol, J.A. TGF-beta stimulation and inhibition of cell proliferation: new mechanistic insights. Cell **63,** 245, 1990.

49. Goodman, L.V., and Majack, R.A. Vascular smooth muscle cells express distinct transforming growth factor-beta receptor phenotypes as a function of cell density in culture. J Biol Chem **264,** 5241, 1989.

50. Majack, R.A. Beta-type transforming growth factor specifies organizational behavior in vascular smooth muscle cell cultures. J Cell Biol **105,** 465, 1987.

51. Serini, G., and Gabbiani, G. Mechanisms of myofibroblast activity and phenotypic modulation. Exp Cell Res **250,** 273, 1999.

52. Darby, I.A., and Hewitson, T.D. Fibroblast differentiation in wound healing and fibrosis. Int Rev Cytol **257,** 143, 2007.

53. Phan, S.H. The myofibroblast in pulmonary fibrosis. Chest **122,** 286S, 2002.

54. Grinnell, F. Fibroblasts, myofibroblasts, and wound contraction. J Cell Biol **124,** 401, 1994.

55. Eikmans, M., Baelde, J.J., de Heer, E., and Bruijn, J.A. ECM homeostasis in renal diseases: a genomic approach. J Pathol **200,** 526, 2003.

56. Iwano, M., and Neilson, E.G. Mechanisms of tubulointerstitial fibrosis. Curr Opin Nephrol Hypertens **13,** 279, 2004.

57. Ronty, M.J., Leivonen, S.K., Hinz, B., Rachlin, A., Otey, C.A., Kahari, V.M., *et al.* Isoform-specific regulation of the actin-organizing protein palladin during TGF-beta1-induced myofibroblast differentiation. J Invest Dermatol **126,** 2387, 2006.

58. Garrett, Q., Khaw, P.T., Blalock, T.D., Schultz, G.S., Grotendorst, G.R., and Daniels, J.T. Involvement of CTGF in TGF-beta1-stimulation of myofibroblast differentiation and collagen matrix contraction in the presence of mechanical stress. Invest Ophthalmol Vis Sci **45,** 1109, 2004.

59. Rosenbaum, J., Blazejewski, S., Preaux, A.M., Mallat, A., Dhumeaux, D., and Mavier, P. Fibroblast growth factor 2 and transforming growth factor beta 1 interactions in human liver myofibroblasts. Gastroenterology **109,** 1986, 1995.

60. Wells, R.G., and Discher, D.E. Matrix elasticity, cytoskeletal tension, and TGF-beta: the insoluble and soluble meet. Sci Signal **1,** pe13, 2008.

61. Wynn, T.A. Cellular and molecular mechanisms of fibrosis. J Pathol **214,** 199, 2008.

62. Rousseau, B., Hirano, S., Chan, R.W., Welham, N.V., Thibeault, S.L., Ford, C.N., *et al.* Characterization of chronic vocal fold scarring in a rabbit model. J Voice **18,** 116, 2004.

63. Tateya, T., Tateya, I., Sohn, J.H., and Bless, D.M. Histologic characterization of rat vocal fold scarring. Ann Otol Rhinol Laryngol **114,** 183, 2005.

64. Hirano, S., Bless, D.M., Rousseau, B., Welham, N., Scheidt, T., and Ford, C.N. Fibronectin and adhesion molecules on canine scarred vocal folds. Laryngoscope **113,** 966, 2003.

65. Gomez, D.E., Alonso, D.F., Yoshiji, H., and Thorgeirsson, U.P. Tissue inhibitors of metalloproteinases: structure, regulation and biological functions. Eur J Cell Biol **74,** 111, 1997.

66. Attisano, L., Wrana, J.L., Lopez-Casillas, F., and Massague, J. TGF-beta receptors and actions. Biochim Biophys Acta **1222,** 71, 1994.

67. Wrana, J.L., Attisano, L., Wieser, R., Ventura, F., and Massague, J. Mechanism of activation of the TGF-beta receptor. Nature **370,** 341, 1994.

68. Nakao, A., Imamura, T., Souchelnytskyi, S., Kawabata, M., Ishisaki, A., Oeda, E., *et al.* TGF-beta receptor-mediated signalling through Smad2, Smad3 and Smad4. EMBO J **16,** 5353, 1997.

Address correspondence to:
Susan L. Thibeault, Ph.D.
Division of Otolaryngology-Head and Neck Surgery
Department of Surgery
University of Wisconsin Madison
5107 WIMR
1111 Highland Ave
Madison, WI 53705-2275

E-mail: thibeault@surgery.wisc.edu